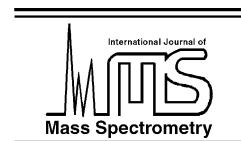




ELSEVIER

International Journal of Mass Spectrometry 218 (2002) 301–304



www.elsevier.com/locate/ijms

Subject index Volume 218

Absolute cross-sections

N^+ charge transfer in N_2 at low-keV collisions, 161

Accelerator mass spectrometry

A new accelerator mass spectrometry system for ^{14}C -quantification of biochemical samples, 255

Acetic acid–benzene

Comparative study of the binary clusters of acetic acid–water and acetic acid–benzene using electron impact and multiphoton ionization techniques, 49

Acetic acid–water

Comparative study of the binary clusters of acetic acid–water and acetic acid–benzene using electron impact and multiphoton ionization techniques, 49

Acrolein

Theoretical studies on the isomerization and dissociation of the acrolein ions, 19

The dissociation dynamics and thermochemistry of the acrolein ion studied by threshold photoelectron–photoion coincidence spectroscopy, 37

Alkenes

A selected ion flow tube (SIFT), study of the reactions of H_3O^+ , NO^+ and O_2^+ ions with a series of alkenes; in support of SIFT-MS, 87

Angular distributions

N^+ charge transfer in N_2 at low-keV collisions, 161

Aryl cation

Gas phase ion chemistry of *para* substituted benzene diazonium ions, their salt clusters and their related phenyl cations, 131

Aryl diazonium ions

Gas phase ion chemistry of *para* substituted benzene diazonium ions, their salt clusters and their related phenyl cations, 131

Association

A selected ion flow tube (SIFT), study of the reactions of H_3O^+ , NO^+ and O_2^+ ions with a series of alkenes; in support of SIFT-MS, 87

A selected ion flow tube, SIFT, study of the reactions of H_3O^+ , NO^+ and O_2^+ ions with a series of diols, 227

Atomic weight

Absolute isotopic composition and atomic weight of samarium, 167

Beam cooling

Cooling beams of negative ions, 199

Binary mixtures

Secondary ions produced by 400 eV He^+ ion impact on solid films composed of binary mixtures of Ar/Xe, Ar/ N_2 , and Ar/ O_2 at 7 K, 173

Biochemical ^{14}C quantification

A new accelerator mass spectrometry system for ^{14}C -quantification of biochemical samples, 255

Buffer gas

Cooling beams of negative ions, 199

Carbon dioxide

High accuracy method for isotope dilution mass spectrometry with application to the measurement of carbon dioxide, 63

Carbon tetrafluoride

Fragmentation of CF_4^{2+} dication from threshold to 120 eV, 11

$C_3H_3^+$ isomers

Interaction of $C_3H_3^+$ isomers with molecular nitrogen: IR spectra of $C_3H_3^+-(N_2)_n$ clusters ($n = 1-6$), 281

$C_3H_3^+-(N_2)_n$ clusters

Interaction of $C_3H_3^+$ isomers with molecular nitrogen: IR spectra of $C_3H_3^+-(N_2)_n$ clusters ($n = 1-6$), 281

Charge transfer

A selected ion flow tube (SIFT), study of the reactions of H_3O^+ , NO^+ and O_2^+ ions with a series of alkenes; in support of SIFT-MS, 87

N^+ charge transfer in N_2 at low-keV collisions, 161

A selected ion flow tube, SIFT, study of the reactions of H_3O^+ , NO^+ and O_2^+ ions with a series of diols, 227

Charged-particle beams

A new accelerator mass spectrometry system for ^{14}C -quantification of biochemical samples, 255

Charge-exchange

A new accelerator mass spectrometry system for ^{14}C -quantification of biochemical samples, 255

Chloroform

A novel electron source for negative ion mobility spectrometry, 75

CID

Gas phase ion chemistry of *para* substituted benzene diazonium ions, their salt clusters and their related phenyl cations, 131

Cluster ion

Ion rearrangement at the beginning of cluster formation: isomerization pathways and dissociation kinetics for the ionized dimethylamine dimer, 1

Clusters

Comparative study of the binary clusters of acetic acid–water and acetic acid–benzene using electron impact and multiphoton ionization techniques, 49

Cooler quadrupole

Cooling beams of negative ions, 199

Cyclic dimers

Comparative study of the binary clusters of acetic acid–water and acetic acid–benzene using electron impact and multiphoton ionization techniques, 49

 D_3^+

Advanced integrated stationary afterglow method for experimental study of recombination of processes of H_3^+ and D_3^+ ions with electrons, 105

Density functional theory

Ion rearrangement at the beginning of cluster formation: isomerization pathways and dissociation kinetics for the ionized dimethylamine dimer, 1

Detection efficiency

Pulse-height distribution of output signals in positive ion detection by a microchannel plate, 237

DFT calculations

Theoretical studies on the isomerization and dissociation of the acrolein ions, 19

Dianions

The influence of the trapping potential on the attachment of a second electron to stored metal cluster and fullerene anions, 217

Dication

Fragmentation of CF_4^{2+} dication from threshold to 120 eV, 11

Diols

A selected ion flow tube, SIFT, study of the reactions of H_3O^+ , NO^+ and O_2^+ ions with a series of diols, 227

Dissociation

Theoretical studies on the isomerization and dissociation of the acrolein ions, 19

The dissociation dynamics and thermochemistry of the acrolein ion studied by threshold photoelectron–photoion coincidence spectroscopy, 37

A selected ion flow tube (SIFT), study of the reactions of H_3O^+ , NO^+ and O_2^+ ions with a series of alkenes; in support of SIFT-MS, 87

A selected ion flow tube, SIFT, study of the reactions of H_3O^+ , NO^+ and O_2^+ ions with a series of diols, 227

Electron affinity

A theoretical study of high electron affinity sulfur oxyfluorides: SO_3F , SO_2F_3 , and SOF_5 , 207

ESI/MS

Gas phase ion chemistry of *para* substituted benzene diazonium ions, their salt clusters and their related phenyl cations, 131

Fourier-transform ion cyclotron resonance (FT-ICR)

The influence of the trapping potential on the attachment of a second electron to stored metal cluster and fullerene anions, 217

Fragmentation

Fragmentation of CF_4^{2+} dication from threshold to 120 eV, 11

Fullerenes

The influence of the trapping potential on the attachment of a second electron to stored metal cluster and fullerene anions, 217

G2 theory

A theoretical study of high electron affinity sulfur oxyfluorides: SO_3F , SO_2F_3 , and SOF_5 , 207

 H_3^+

Advanced integrated stationary afterglow method for experimental study of recombination of processes of H_3^+ and D_3^+ ions with electrons, 105

Harmonic balance method

Transition curves and *iso- β_u* lines in nonlinear Paul traps, 181

IMS

Reverse flow continuous corona discharge ionisation applied to ion mobility spectrometry, L1

Inductively coupled plasma mass spectrometry

Precise isotope analysis of natural and enriched osmium samples using different ICP-MS instruments, 245

Intermolecular potential

Interaction of $C_3H_3^+$ isomers with molecular nitrogen: IR spectra of $C_3H_3^+-(N_2)_n$ clusters ($n = 1-6$), 281

Interstellar ions

Advanced integrated stationary afterglow method for experimental study of recombination of processes of H_3^+ and D_3^+ ions with electrons, 105

Ion branching ratios

Fragmentation of CF_4^{2+} dication from threshold to 120 eV, 11

Ion impact

Secondary ions produced by 400 eV He^+ ion impact on solid films composed of binary mixtures of Ar/Xe, Ar/ N_2 , and Ar/ O_2 at 7 K, 173

Ion mobility spectrometry

A novel electron source for negative ion mobility spectrometry, 75

Ionic complexes

Interaction of $C_3H_3^+$ isomers with molecular nitrogen: IR spectra of $C_3H_3^+-(N_2)_n$ clusters ($n = 1-6$), 281

Ion–molecule reactions

Gas phase ion chemistry of *para* substituted benzene diazonium ions, their salt clusters and their related phenyl cations, 131

IR spectroscopy

Interaction of $C_3H_3^+$ isomers with molecular nitrogen: IR spectra of $C_3H_3^+-(N_2)_n$ clusters ($n = 1-6$), 281

Isomerization

Theoretical studies on the isomerization and dissociation of the acrolein ions, 19

Isotope dilution mass spectrometry (IDMS)

High accuracy method for isotope dilution mass spectrometry with application to the measurement of carbon dioxide, 63

Isotope ratio mass spectrometry

High accuracy method for isotope dilution mass spectrometry with application to the measurement of carbon dioxide, 63

Isotope ratio measurement

Precise isotope analysis of natural and enriched osmium samples using different ICP-MS instruments, 245

- Isotopic abundance
 Absolute isotopic composition and atomic weight of samarium, 167
- Mass spectrometry
 Reverse flow continuous corona discharge ionisation applied to ion mobility spectrometry, L1
 Absolute isotopic composition and atomic weight of samarium, 167
- MCP
 Pulse-height distribution of output signals in positive ion detection by a microchannel plate, 237
- Metal clusters
 The influence of the trapping potential on the attachment of a second electron to stored metal cluster and fullerene anions, 217
- Microsolvation
 Interaction of $C_3H_3^+$ isomers with molecular nitrogen: IR spectra of $C_3H_3^+(N_2)_n$ clusters ($n = 1-6$), 281
- Molecular ion dissociation
 A new accelerator mass spectrometry system for ^{14}C -quantification of biochemical samples, 255
- Multiphoton ionization
 Comparative study of the binary clusters of acetic acid–water and acetic acid–benzene using electron impact and multiphoton ionization techniques, 49
- N^+
 N^+ charge transfer in N_2 at low-keV collisions, 161
- Negative corona discharge
 A novel electron source for negative ion mobility spectrometry, 75
- Negative ions
 Cooling beams of negative ions, 199
- Nitrobenzene
 A novel electron source for negative ion mobility spectrometry, 75
- NO_x
 Reverse flow continuous corona discharge ionisation applied to ion mobility spectrometry, L1
- Nonlinear Mathieu equation
 Transition curves and $iso-\beta_u$ lines in nonlinear Paul traps, 181
- Nonlinear Paul traps
 Transition curves and $iso-\beta_u$ lines in nonlinear Paul traps, 181
- Osmium
 Precise isotope analysis of natural and enriched osmium samples using different ICP-MS instruments, 245
- Ozone
 Reverse flow continuous corona discharge ionisation applied to ion mobility spectrometry, L1
- Penning trap
 The influence of the trapping potential on the attachment of a second electron to stored metal cluster and fullerene anions, 217
- Photoionization mass spectra
 The dissociation dynamics and thermochemistry of the acrolein ion studied by threshold photoelectron–photoion coincidence spectroscopy, 37
- Plasma
 Advanced integrated stationary afterglow method for experimental study of recombination of processes of H_3^+ and D_3^+ ions with electrons, 105
- Positive ion
 Pulse-height distribution of output signals in positive ion detection by a microchannel plate, 237
- Proton transfer
 A selected ion flow tube (SIFT), study of the reactions of H_3O^+ , NO^+ and O_2^+ ions with a series of alkenes; in support of SIFT-MS, 87
 A selected ion flow tube, SIFT, study of the reactions of H_3O^+ , NO^+ and O_2^+ ions with a series of diols, 227
- Pulse-height distribution
 Pulse-height distribution of output signals in positive ion detection by a microchannel plate, 237
- Recombination
 Advanced integrated stationary afterglow method for experimental study of recombination of processes of H_3^+ and D_3^+ ions with electrons, 105
- RRKM
 Ion rearrangement at the beginning of cluster formation: isomerization pathways and dissociation kinetics for the ionized dimethylamine dimer, 1
- Samarium
 Absolute isotopic composition and atomic weight of samarium, 167
- Secondary ions
 Secondary ions produced by 400 eV He^+ ion impact on solid films composed of binary mixtures of Ar/Xe, Ar/ N_2 , and Ar/ O_2 at 7 K, 173
- SIFT
 A selected ion flow tube (SIFT), study of the reactions of H_3O^+ , NO^+ and O_2^+ ions with a series of alkenes; in support of SIFT-MS, 87
 A selected ion flow tube, SIFT, study of the reactions of H_3O^+ , NO^+ and O_2^+ ions with a series of diols, 227
- SO_2F_3
 A theoretical study of high electron affinity sulfur oxyfluorides: SO_3F , SO_2F_3 , and SOF_5 , 207
- SO_3F
 A theoretical study of high electron affinity sulfur oxyfluorides: SO_3F , SO_2F_3 , and SOF_5 , 207
- SOF_5
 A theoretical study of high electron affinity sulfur oxyfluorides: SO_3F , SO_2F_3 , and SOF_5 , 207
- Solid films
 Secondary ions produced by 400 eV He^+ ion impact on solid films composed of binary mixtures of Ar/Xe, Ar/ N_2 , and Ar/ O_2 at 7 K, 173
- Stationary afterglow
 Advanced integrated stationary afterglow method for experimental study of recombination of processes of H_3^+ and D_3^+ ions with electrons, 105

Sulfur oxyfluoride

A theoretical study of high electron affinity sulfur oxyfluorides: SO_3F , SO_2F_3 , and SOF_5 , 207

Synchrotron radiation

Fragmentation of CF_4^{2+} dication from threshold to 120 eV, 11

Thermochemistry

Theoretical studies on the isomerization and dissociation of the acrolein ions, 19

The dissociation dynamics and thermochemistry of the acrolein ion studied by threshold photoelectron–photoion coincidence spectroscopy, 37

TPEPICO

The dissociation dynamics and thermochemistry of the acrolein

ion studied by threshold photoelectron–photoion coincidence spectroscopy, 37

Transition curves and $iso-\beta_u$ lines

Transition curves and $iso-\beta_u$ lines in nonlinear Paul traps, 181

Trinitrotoluene

A novel electron source for negative ion mobility spectrometry, 75

Two-step IDMS

High accuracy method for isotope dilution mass spectrometry with application to the measurement of carbon dioxide, 63

Unimolecular decomposition

Ion rearrangement at the beginning of cluster formation: isomerization pathways and dissociation kinetics for the ionized dimethylamine dimer, 1